Progress In Electromagnetics Research M, Vol. 102, 159–169, 2021

A Novel Triple Band MIMO Antenna Array for Simultaneous Communications

Jangampally Rajeshwar Goud[1, *], Nalam V. Koteswara Rao[2], and Avala M. Prasad[3]

Abstract—A novel and compact triple-band two-element Multiple Input Multiple Output (MIMO) antenna array is designed to provide simultaneous communications for uplink and downlink which covers GSM, LTE, and sub-6 base station applications. The proposed MIMO system is a configuration of four triple-band two-element arrays in which two are used for uplink and the other two for downlink. This compact structure with separate antennas for uplink and downlink provides simultaneous communication. For this proposed structure, the parameters like impedance bandwidth, efficiency, gain, and cross polarization aspects are presented for all the three specified bands. To achieve good isolation, uplink and downlink arrays are placed orthogonal to each other. Further, to enhance the isolation a defected ground is incorporated for the antenna array structure, and isolation strips are provided between uplink and downlink arrays. In addition, for the proposed structure diversity performance with Envelope Correlation Coefficient (ECC) and diversity gains are also calculated. The simulated and measured results are in acceptable correlation.

1. INTRODUCTION

MIMO antenna systems are absolutely necessary to provide high data rate and good channel capacity for present mobile communications. Peculiarly, base stations need multiband antennas to cover 2G/3G/LTE (4G)/5G bands, which drives researchers to develop multiband MIMO antenna systems [1]. A great deal of research has been carried out towards developing multi-broadband and narrow band MIMO antennas to cover these frequency bands. Broadband can be achieved using folded dipoles [2]. Dual broadbands are accomplished by a pair of folded dipoles with parasitic elements [3], orthogonal dipoles [4], trapezoidal dipoles [5], inverted π- and L-shaped antennas [6], and a magnetoelectric dipole [7]. Triple broadbands are reported using a pair of rings with arrow-shaped dipoles [8] and a coupled-fed strip with a parasitic arm [9].

Triple narrow bands are obtained with meander-line type inverted-L [10] and meander structure [11]. In these models, isolation is provided for uplink and downlink communications using guard period, guard band, and discontinuous transmission. To minimize the interference, the base stations need to be synchronized [12]. To address the problems of discontinuous transmission and interference, multi narrow band antennas are in demand for achieving simultaneous communications for uplink and downlink. Studies are reported [13] to provide simultaneous communications by using two independent U-slot rectangular microstrip antennas.

The performance of MIMO systems also relies on the mutual coupling between the elements. Many coupling reduction techniques have been reported using parallel coupled resonators [14], F-shaped stubs in ground plane [15], fractal electromagnetic band gaps [16], two planar-monopole antenna elements [17],

Received 22 April 2021, Accepted 14 May 2021, Scheduled 19 May 2021

* Corresponding author: Jangampally Rajeshwar Goud (rajeshwargoud@gmail.com).

[1] ECE Department, Jawaharlal Nehru Technological University, Kakinada, Andhra Pradesh, India. [2] ECE Department, Chaitanya Bharathi Institute of Technology, Hyderabad, Telangana, India. [3] ECE Department, University College of Engineering, Jawaharlal Nehru Technological University, Kakinada, Andhra Pradesh, India.

an S-shaped EBG structure [18], and a parasitic element structure with a single complementary split ring resonator [19]. Consequently, it is noticed that there is a need for miniaturized multi narrow band MIMO antennas for simultaneous communications with good isolation between the elements.

In this paper, the configuration of four triple-band two-element MIMO antenna arrays is proposed for simultaneous communications. The detailed explanation of design and structure of the proposed antenna and its feeding structure are also presented. Results and diversity performance of the proposed MIMO array are discussed.

2. ANTENNA DESIGN AND STRUCTURE

2.1. Antenna Array Geometry

The geometry of a triple-band two-element array is shown in Figure 1. Initially, single triple-band antenna is designed on FR4 ($\epsilon_r = 4.4$) with substrate height (h) 1.6 mm, which covers GSM1800, LTE2600, and sub-6 frequency bands. The upper band is achieved by choosing the appropriate lengths ($L1, L9$ and $L10$) as shown in case I of Figure 2. Middle band is obtained by adding additional lengths ($L2$, $L6$, $L7$, and $L8$) to $L1$ as shown in case II of Figure 2. Case III of the same figure illustrates how lower band is achieved by adding lengths ($L2$, $L3$, $L4$, and $L5$) to $L1$. In the respective three bands, the

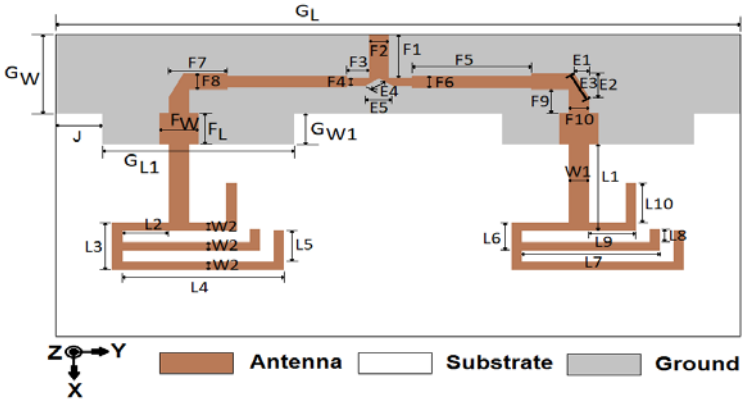

Figure 1. Triple-band two-element array. Dimensions — Downlink antenna (in mm): $L1 = 11$, $L2 = 5$, $L3 = 6$, $L4 = 17$, $L5 = 2$, $L6 = 3.5$, $L7 = 14.5$, $L8 = 1.5$, $L9 = 5$, $L10 = 5$, $W1 = 2$, $W2 = 1$, $F_L = 4$, $F_W = 4$, $F1 = 5.5$, $F2 = 2$, $F3 = 7$, $F4 = 1$, $F5 = 12.5$, $F6 = 1.5$, $F7 = 6$, $F8 = 2$, $F9 = 3$, $F10 = 2$, $E1 = 1.5$, $E2 = 3$, $E3 = 3.35$, $E4 = 1.8$, $E5 = 3$, $J = 5$, $G_{L1} = 20$, $G_{W1} = 4$, $G_L = 72$, $G_W = 10$. Uplink antenna (in mm): $L1 = 11$, $L2 = 5$, $L3 = 6$, $L4 = 17$, $L5 = 4$, $L6 = 3.5$, $L7 = 14.5$, $L8 = 1.7$, $L9 = 5$, $L10 = 5$, $W1 = 2$, $W2 = 1$, $F_L = 4$, $F_W = 4$, $F1 = 5.5$, $F2 = 2$, $F3 = 7$, $F4 = 1$, $F5 = 12.5$, $F6 = 1.5$, $F7 = 6$, $F8 = 2$, $F9 = 3$, $F10 = 2$, $E1 = 1.5$, $E2 = 3$, $E3 = 3.35$, $E4 = 1.8$, $E5 = 3$, $J = 5$, $G_{L1} = 20$, $G_{W1} = 4$, $G_L = 72$, $G_W = 10$.

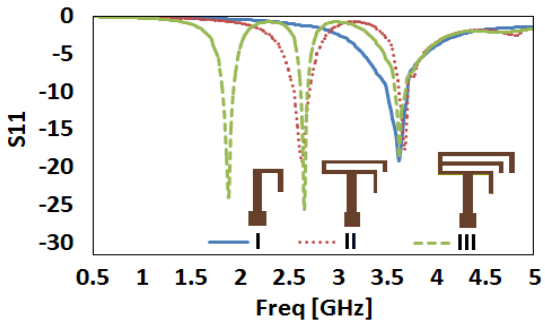

Figure 2. Return loss of triple band MIMO array.

Table 1. Power divider dimensions of uplink and downlink arrays.

Parameter	Value (mm)
Length of 50 Ω microstrip line ($F1$)	0.047λ
Width of 50 Ω microstrip line ($F2$)	0.017λ
Length of 100 Ω microstrip line ($F3$)	0.06λ
Width of 100 Ω microstrip line ($F4$)	0.0086λ
Length of 70.7 Ω microstrip line ($F5$)	0.108λ
Width of 70.7 Ω microstrip line ($F6$)	0.013λ
Length of 50 Ω microstrip line ($F7$)	0.052λ
Width of 50 Ω microstrip line ($F8$)	0.017λ
Length of 50 Ω microstrip line ($F9$)	0.026λ
Width of 50 Ω microstrip line ($F10$)	0.017λ

resonance is obtained when the individual strip length in each case is approximately equal to quarter wavelength. A compact structure is achieved by bending the strips. The exact resonant frequency is achieved by varying the length of the strip, and the impedance matching is accomplished by adjusting the width of the strip (W). The antenna feeds with a microstrip line having length (F_L) and width (F_W). Beneath the microstrip line, the ground plane is provided with length (G_{L1}) and width (G_{W1}).

To improve the gain and directivity, a two-element array is designed which is shown in Figure 1. The spacing between the elements is considered approximately half wavelength for upper band, one third wavelength for middle band, and quarter wavelength for lower band. Corporate feeding technique is employed for the array. The feed network is designed by using T-shaped power dividers such that equal amplitude with equal phase is fed to the antenna elements. Quarter wave transformers and also mitering the corners of the bends are used for impedance matching. Power divider dimensions of uplink and downlink arrays are shown in Table 1 and are indicated in terms of λ (Wavelength of middle band). Beneath the corporate feed the ground plane is printed with length (G_L) and width (G_W).

2.2. MIMO Array Geometry

To meet the requirement of simultaneous communications, it is required to design the uplink and downlink antennas separately. Desired frequencies of uplink and downlink communications are obtained by considering the proper length of strips. The proposed MIMO antenna consists of four triple-band

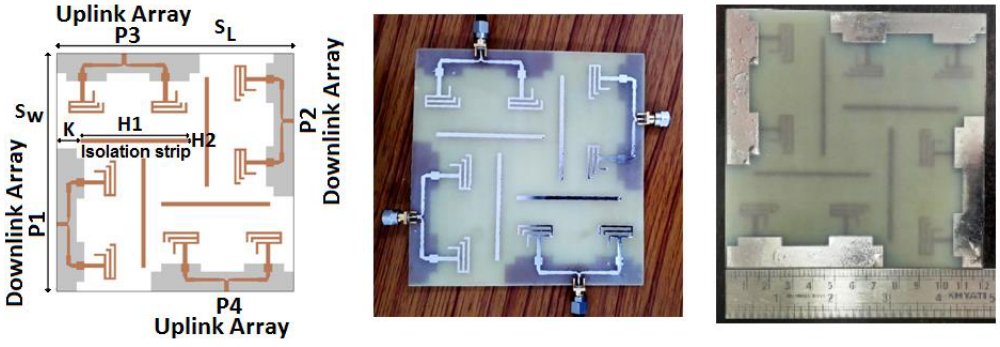

Figure 3. Triple band two element MIMO antenna array. (a) Geometry. (b) Fabricated antenna (top view). (c) Fabricated antenna (bottom view). Dimensions (in mm): $S_L = 120$, $S_W = 120$, $H1 = 55$, $H2 = 2$, $K = 12$.

two-element antenna arrays in which two are used for uplink and the other two for downlink as shown in Figure 3. Ports P1 and P2 are assigned for downlink MIMO antenna arrays and ports P3 and P4 assigned for uplink MIMO antenna arrays. The proposed antenna simulation results are carried out using HFSS, and its structure is fabricated on an FR4 substrate (120 mm × 120 mm) with height 1.6 mm.

As shown in Figure 3, ports P1 and P2 of downlink antenna arrays are diagonally located. Similarly, ports P3 and P4 of uplink antenna arrays are also placed. Further, ports P1, P3 and P2, P4 are right angle to each other. Isolation strips are placed for reducing the mutual coupling between these uplink and downlink antenna arrays which also results in an improved diversity performance. The triple-band two-element MIMO antenna array geometry and fabricated antenna are shown in Figure 3. The proposed MIMO antenna array is easy to integrate with the practical system of relevant applications due to its compact and planar structure.

3. RESULTS AND DISCUSSION

3.1. Downlink MIMO Antenna Array

The triple-band downlink antenna array is designed to operate in GSM1800, LTE2600, and sub-6 bands. The ranges of frequencies 1805–1880 MHz and 2620–2690 MHz are used for downlink communication in the first (GSM1800) and second (LTE2600) bands, respectively [20]. The third band (sub-6 n78 NR) with frequency range 3300–3800 MHz is used for 5G uplink and downlink communications. Reflection coefficients of all the ports are measured using KEYSIGHT N9915A Microwave Analyzer. The return loss of downlink array is obtained by exciting port P1 and terminating all the other ports. The simulated impedance bandwidths of the first, second, and third bands are obtained at 1790–1900 MHz, 2625–2670 MHz, and 3500–3690 MHz, respectively; however, the measured impedance bandwidths for same bands are obtained at 1810–1920 MHz, 2650–2720 MHz, and 3510–3720 MHz which can be seen in Figure 4. More than 70 MHz bandwidth is achieved in all the specified bands which are listed in Table 2.

Simulated and measured radiation patterns of downlink antenna array are plotted at 1.85 GHz, 2.65 GHz, and 3.65 GHz as shown in Figure 7. Radiation patterns are obtained in far field region in which horn antenna is used for transmission, and proposed antenna is used for reception. These patterns are obtained when port P1 is used for reception, and all other ports are terminated with matched load. The simulated and measured total gain patterns are plotted at $\Phi = 0°$ and $\Phi = 90°$. The simulated half power beam widths 73°, 68°, 62° and measured 51°, 46°, 43° are achieved at 1.85 GHz, 2.65 GHz, and 3.65 GHz, respectively. Similarly, efficiencies 65.74%, 69.26%, 74.76% are obtained in simulation and 63.56%, 67.32%, 72.58% in measured results. Cross polarizations are more than 23 dBi, 20 dBi, and 18 dBi in both results. The peak gains are listed in Table 2. Gain verses frequency plot of downlink antenna array is shown in Figure 6.

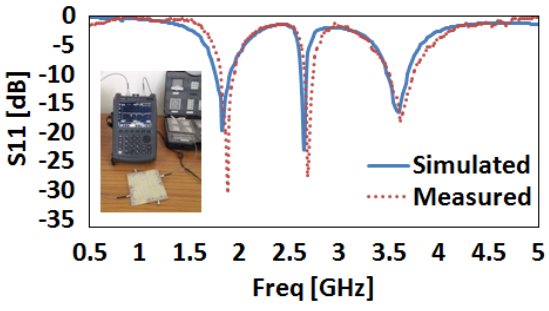

Figure 4. Return loss of triple band downlink MIMO antenna array.

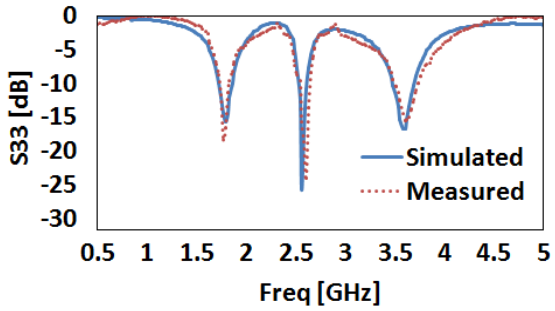

Figure 5. Return loss of triple band uplink MIMO antenna array.

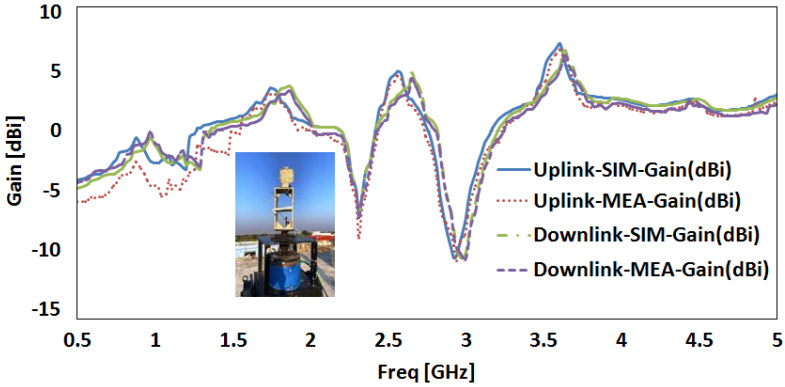

Figure 6. Gain versus frequency of uplink and downlink MIMO array.

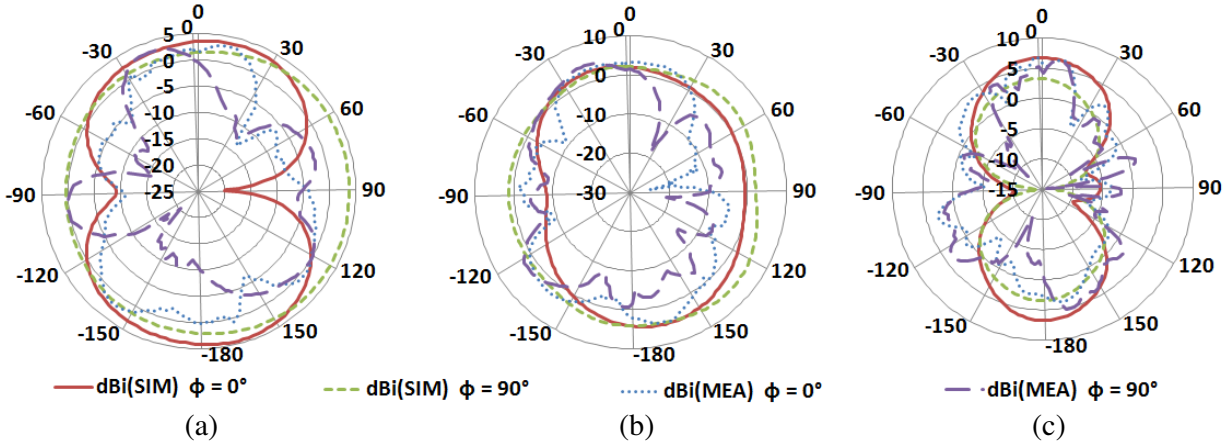

Figure 7. Radiation patterns of downlink antenna array. (a) 1.85 GHz, (b) 2.65 GHz, (c) 3.65 GHz.

3.2. Uplink MIMO Antenna Array

The triple-band uplink antenna array is designed to operate in GSM1800, LTE2600, and sub-6 bands. The ranges of frequencies 1710–1785 MHz and 2500–2570 MHz are used for uplink communication in the first and second bands, respectively [20]. The return loss of uplink array is obtained by exciting port P3 and terminating all the other ports. The simulated impedance bandwidths of the first, second, and third bands are obtained at 1720–1800 MHz, 2530–2600 MHz, and 3480–3690 MHz, respectively, where the measured impedance bandwidths for the same bands are obtained at 1740–1810 MHz, 2540–2620 MHz, and 3500–3710 MHz which can be seen in Figure 5. More than 70 MHz bandwidth is obtained in all three specified bands.

Simulated and measured radiation patterns of uplink antenna array are plotted at 1.75 GHz, 2.55 GHz, and 3.55 GHz as shown in Figure 8. The simulated and measured total gain patterns are plotted at $\Phi = 0°$ and $\Phi = 90°$.

The simulated half power beam widths 74°, 66°, 61° and measured 53°, 47°, 42° are achieved at 1.75 GHz, 2.65 GHz, and 3.55 GHz, respectively. Similarly, efficiencies 65.21%, 70.42%, 75.83% are obtained in simulation and 63.24%, 68.38%, 73.29% in measured results. Cross polarizations are more than 22 dBi, 20 dBi, and 17 dBi in both results. The peak gains are listed in Table 2. Gain verses frequency plot of uplink antenna array is shown in Figure 6.

In downlink antenna array, port-1 is excited, and all other ports are terminated with matched load. The surface current is distributed in $L1$, $L9$, and $L10$ strips when the antenna resonates at upper band which is shown in Figure 9(a). Similarly when the antenna resonates at middle band and upper band,

Table 2. Comparison between proposed antenna and triple band antennas.

Ref.	Size (mm) ($L \times W \times h$)	Freq.	Band Width (MHz)	Isolation (dB)	ECC	Gain (dBi)
[8]	$152 \times 152 \times 12$	f_1: 2.4 f_2: 3.5 f_3: 5	BW_1: 100 BW_2: 300 BW_3: 800	> 20	< 0.1	f_1: 7.5 f_2: 8.2 f_3: 9.3
[9]	$150 \times 75 \times 3.8$	f_1: 3.5 f_2: 5.5 f_3: 5.9	BW_1: 500 BW_2: 200 BW_3: 775	> 10.5	< 0.12	f_1: 3.2 f_2: 3.5 f_3: 4.2
[10]	$100 \times 65 \times 1.6$	f_1: 0.9 f_2: 1.8 f_3: 2.6	BW_1: 30 BW_2: 50 BW_3: 280	> 11	< 0.7	f_1: 0.25 f_2: 0.60 f_3: 3.28
[11]	$42 \times 15 \times 1.6$	f_1: 0.9 f_2: 1.8 f_3: 2.4	BW_1: 30 BW_2: 40 BW_3: 30	NG	NG	f_1: 1.6 f_2: 2.1 f_3: 1.9
[13]	$70 \times 130 \times 1.6$	f_{1U}: 0.82 f_{2U}: 1.74 f_{3U}: 2.34 f_{1D}: 0.88 f_{2D}: 1.83 f_{3D}: 2.35	BW_1: 9 BW_2: 23 BW_3: 34 BW_1: 8 BW_2: 40 BW_3: 37	> 20	< 0.02	f_{1U}: 2.26 f_{2U}: 3.42 f_{3U}: 2.84 f_{1D}: 1.62 f_{2D}: 2.36 f_{3D}: 2.84
PROPOSED	$120 \times 120 \times 1.6$	f_{1U}: 1.75 f_{2U}: 2.55 f_{3U}: 3.55 f_{1D}: 1.85 f_{2D}: 2.65 f_{3D}: 3.65	BW_1: 70 BW_2: 80 BW_3: 210 BW_1: 110 BW_2: 70 BW_3: 210	> 26	< 0.13	f_{1U}: 3.15 f_{2U}: 4.65 f_{3U}: 6.84 f_{1D}: 3.37 f_{2D}: 4.42 f_{3D}: 6.37

f: Resonance frequency, BW: Band width, NG: Not Given, U: Uplink and D: Downlink

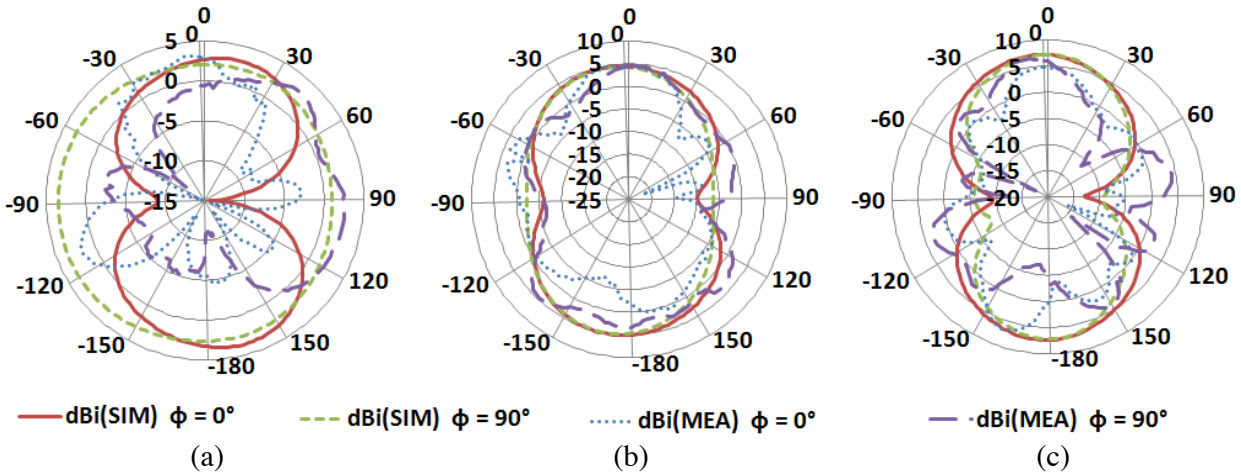

Figure 8. Radiation patterns of uplink antenna array. (a) 1.75 GHz, (b) 2.55 GHz, (c) 3.55 GHz.

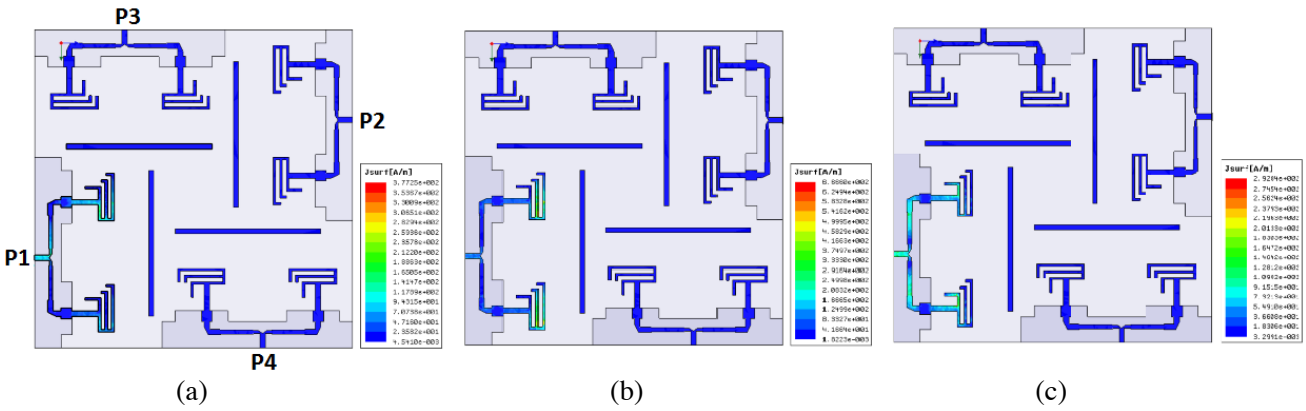

Figure 9. Current distribution of downlink antenna array. (a) 1.85 GHz, (b) 2.65 GHz, (c) 3.65 GHz.

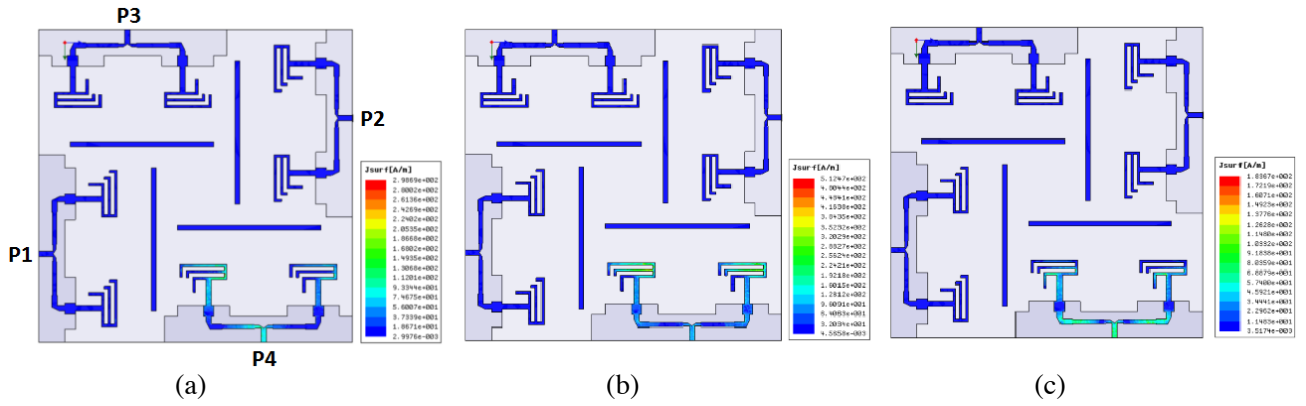

Figure 10. Current distribution of uplink antenna array. (a) 1.75 GHz, (b) 2.55 GHz, (c) 3.55 GHz.

the current is distributed in ($L1$, $L2$, $L6$, $L7$, and $L8$) and ($L1$, $L2$, $L3$, $L4$, and $L5$) strips which are shown in Figures 9(b) and 9(c), respectively. This is explained in detail using three different cases in Section 2.1. In uplink antenna array, port-4 is excited, and all other ports are terminated with matched load; current distribution is observed similar to downlink antenna array which is shown in Figure 10.

3.3. Isolation between MIMO Antenna Arrays

Mutual coupling is an important parameter in MIMO system. The MIMO system requires at least 12 dB isolation between the ports. The two uplink antenna array elements are placed diagonal to each other, and in a similar way, downlink antenna array elements are also placed diagonal to each other whereas uplink and downlink array elements are placed orthogonally to improve the performance of MIMO system. Defected ground plane is used to decouple the array elements. Spacing (J) between the edge of the substrate and location of the ground plane is optimized to reduce the mutual coupling [10].

The isolation between the downlink array elements (i.e., P1 and P2) and uplink array elements (i.e., P3 and P4) is more than 30 dB achieved in simulation. Also, more than 23 dB simulated isolation between uplink array and downlink array is obtained, i.e., (P1 and P3), (P1 and P4), (P3 and P1), and (P3 and P2). Placing isolation strips between the uplink and downlink antenna arrays has experimentally resulted in an isolation of 26 dB. Figure 11 describes the comparison of isolation parameters with and without strips. Spacing (K) between the edge of the substrate and location of the isolation strip is optimized for obtaining a better isolation.

The arrangement of proposed structure without placing the strips in between the arrays is shown in Figure 12(a) where Figure 12(b) shows the arrangement of arrays with strips. The corresponding

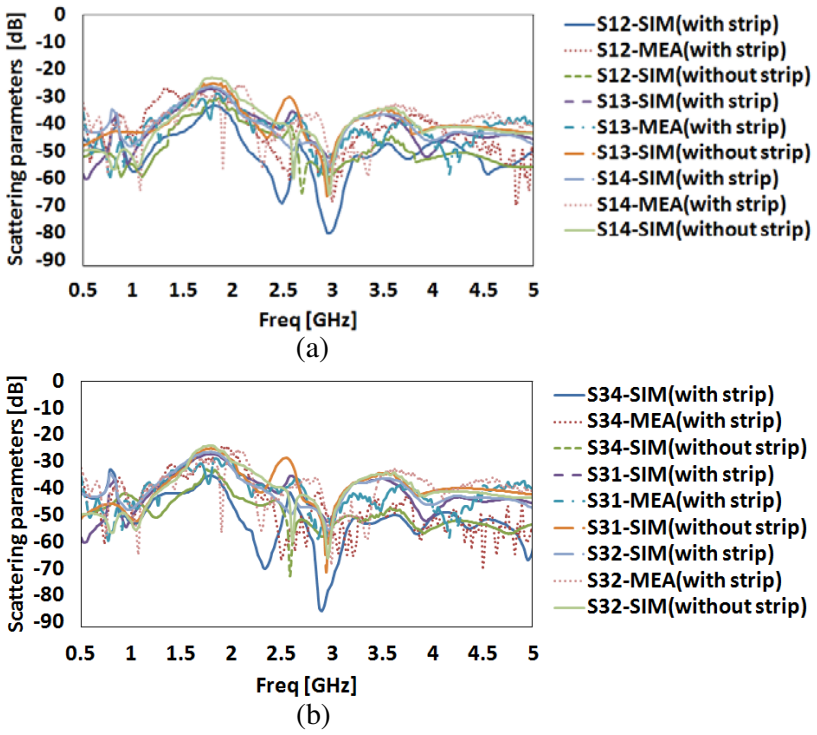

Figure 11. Mutual coupling between the MIMO array elements, (a) S_{12}, S_{13} and S_{14}, (b) S_{34}, S_{31} and S_{32}.

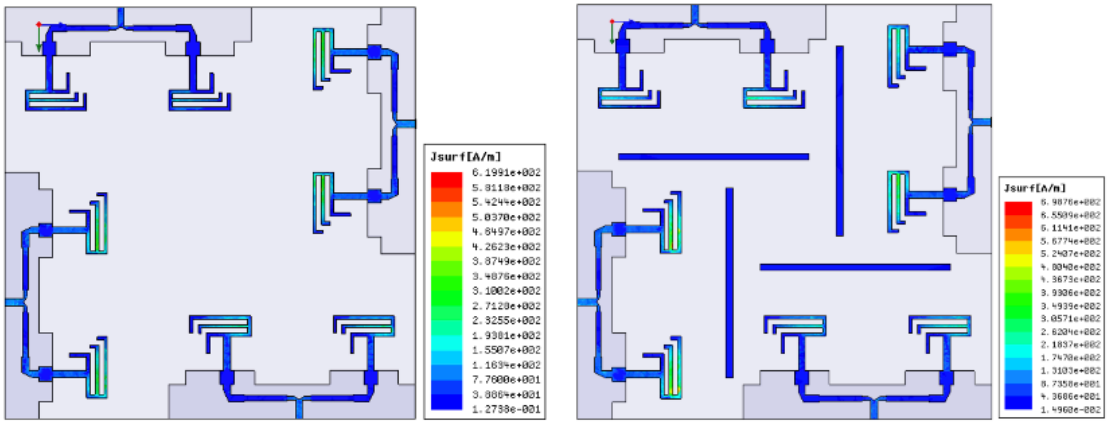

Figure 12. Current distribution of proposed MIMO antenna, (a) without isolation strips and (b) with isolation strips.

surface current distributions are also indicated in the figures. It is noticed that there is an increment of 3 dB isolation by adding isolation strips between the uplink and downlink antenna arrays.

4. DIVERSITY PERFORMANCE OF MIMO ANTENNA ARRAYS

Envelope correlation coefficient (ECC) is a major parameter to estimate the diversity performance of MIMO system. ECC and diversity gain are measured separately for uplink and downlink MIMO antenna arrays. ECC can be calculated using two methods. In the first method, ECC (ρ_e) can be obtained by

mathematically calculating from below expression using measured far field radiation patterns [21].

$$\mathrm{ECC}(\rho_e) = \frac{\left|\oiint_\Omega \left[E_i\left(\theta,\Phi\right)\cdot E_j\left(\theta,\Phi\right)\right] d\Omega\right|^2}{\oiint_\Omega \left[\left|E_{\theta i}\left(\theta,\Phi\right)\right|^2 + \left|E_{\Phi i}\left(\theta,\Phi\right)\right|^2\right] d\Omega \oiint_\Omega \left[\left|E_{\theta j}\left(\theta,\Phi\right)\right|^2 + \left|E_{\Phi j}\left(\theta,\Phi\right)\right|^2\right] d\Omega} \tag{1}$$

where

$$E_i\left(\theta,\Phi\right)\cdot E_j\left(\theta,\Phi\right) = E_{\theta i}\left(\theta,\Phi\right)E^*_{\theta j}\left(\theta,\Phi\right) + E_{\Phi i}\left(\theta,\Phi\right)E^*_{\Phi j}\left(\theta,\Phi\right) \tag{2}$$

E_θ and E_Φ are the electric far field components along elevation (θ) and azimuth (Φ) angles, respectively. For downlink MIMO antenna array, i corresponds to P1, and j corresponds to P2. Similarly for uplink MIMO antenna array, i corresponds to P3, and j corresponds to P4. Electric field components of downlink MIMO antenna array is calculated by exciting P1 and terminating the other ports with matched load. Electric field components of all the other ports are obtained in a similar way, i.e., exciting the respective ports and terminating the remaining ports. The ECC values below 0.13 and diversity gain more than 9.88 dBi are obtained for all three bands of downlink and uplink MIMO antenna arrays.

In the second method, ECCs of downlink and uplink MIMO antenna arrays are obtained using S-parameters [21]. The ECC and diversity gain of uplink and downlink antenna arrays can be calculated mathematically using following expressions.

$$\mathrm{ECC}(\rho_{eD}) = \frac{\left|S^*_{11}S_{12} + S^*_{21}S_{22}\right|^2}{\left(1-\left|S_{11}\right|^2-\left|S_{21}\right|^2\right)\left(1-\left|S_{22}\right|^2-\left|S_{12}\right|^2\right)} \tag{3}$$

$$\mathrm{ECC}(\rho_{eU}) = \frac{\left|S^*_{33}S_{34} + S^*_{43}S_{44}\right|^2}{\left(1-\left|S_{33}\right|^2-\left|S_{43}\right|^2\right)\left(1-\left|S_{44}\right|^2-\left|S_{34}\right|^2\right)} \tag{4}$$

$$\text{Diversity Gain (Downlink)} = 10\sqrt{1-\left|\mathrm{ECC}(\rho_{eD})\right|^2} \tag{5}$$

$$\text{Diversity Gain (Uplink)} = 10\sqrt{1-\left|\mathrm{ECC}(\rho_{eU})\right|^2} \tag{6}$$

The ECC values below 0.05 and diversity gain more than 9.95 dBi are obtained for all three bands of both downlink and uplink MIMO antenna arrays which are shown in Figure 13. In both methods, it is observed that ECC and diversity gain calculations are in the acceptable range [22].

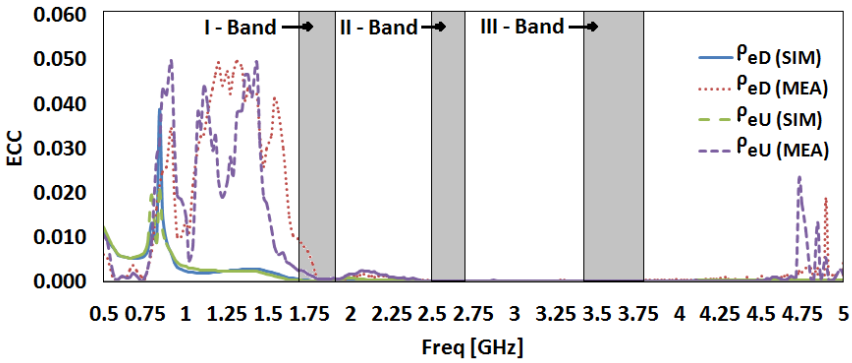

Figure 13. ECC of triple band MIMO antenna array.

5. CONCLUSION

In this paper, a configuration of four triple-band two-element MIMO antenna arrays is presented and finds applications for GSM1800, LTE2600, and sub-6 base stations for the purposes of uplink and downlink communications. Better than −15 dB return loss is achieved in all three bands. Impedance bandwidths of 70 MHz, 80 MHz, and 210 MHz are obtained practically for uplink antenna array whereas

110 MHz, 70 MHz, and 210 MHz are noticed for the downlink antenna arrays, in respective three bands. Further, experimental results show that the proposed antenna array achieves more than 3.15 dBi peak gain, 17 dBi cross polarizations, and 63% efficiencies in all three specified bands. An isolation better than 26 dB is found practically which in turn improves the diversity performance of MIMO system. The calculated ECC values are less than 0.13 in all three bands. The proposed MIMO antenna array is easy to integrate with practical system since it is compact and has planar structure. Simulated and measured results are found in good agreement.

REFERENCES

1. Andrews, J. G., et al., "What will 5G be?" *IEEE Journal on Selected Areas in Communications*, Vol. 3, No. 6, 1065–1082, Jun. 2014, doi: 10.1109/JSA.2014.2328098.
2. Cui, Y., R. Li, and P. Wan, "A novel broadband planar antenna for 2G/3G/LTE base stations," *IEEE Transactions on Antennas and Propagation*, Vol. 6, No. 5, 2767–2774, May 2013, doi: 10.1109/TAP.2013.2244837.
3. Cui, Y., R. Li, and P. Wan, "Novel dual-broadband planar antenna and its array for 2G/3G/LTE base station," *IEEE Transactions on Antennas and Propagation*, Vol. 6, No. 3, 1132–1139, Mar. 2013, doi: 10.1109/TAP.2012.2229377.
4. Huang, H., Y. Liu, and S. Gong, "A novel dual-broadband and dual-polarized antenna for 2G/3G/LTE base stations," *IEEE Transactions on Antennas and Propagation*, Vol. 64, No. 9, 4113–4118, Sept. 2016, doi: 10.1109/TAP.2016.2589966.
5. An, W. X., H. Won, K. L. Lau, S. F. Li, and Q. Xue, "Design of broadband dual-band dipole for base station antenna," *IEEE Transactions on Antennas and Propagation*, Vol. 60, No. 3, 1592–1595, Mar. 201, doi: 10.1109/TAP.2011.2180336.
6. Li, Y., C. Sim, Y. Luo, and G. Yang, "12-port 5G massive MIMO antenna array in sub-6 GHz mobile handset for LTE bands 42/43/46 applications," *IEEE Access*, Vol. 6, 344–354, 2018, doi: 10.1109/ACCESS.2017.2763161.
7. Zhai, H., J. Zhang, Y. Zan, Q. Gao, and C. Liang, "An LTE base-station magnetoelectric dipole antenna with anti-interference characteristics and its MIMO system application," *IEEE Antennas and Wireless Propagation Letters*, Vol. 14, 906–909, 2015, doi: 10.1109/LAW.2014.2384519.
8. Pan, Y., Y. Cui, and R. Li, "Investigation of a triple-band multibeam MIMO antenna for wireless access points," *IEEE Transactions on Antennas and Propagation*, Vol. 64, No. 4, 1234–1241, Apr. 2016, doi: 10.1109/TAP.2016.2526082.
9. Wang, H., R. Zhang, Y. Luo, and G. Yang, "Compact eight-element antenna array for triple-band MIMO operation in 5G mobile terminals," *IEEE Access*, Vol. 8, 19433–19449, 2020, doi: 10.1109/ACCESS.2020.2967651.
10. Sun, J., H. Fan, P. Lin, and C. Chuan, "Triple-band MIMO antenna for mobile wireless application," *IEEE Antennas and Wireless Propagation Letters*, Vol. 15, 500–503, 2016, doi: 10.1109/LAW.2015.2454536.
11. Sun, X.-B., "Design of a triple-band antenna based on its current distribution," *Progress In Electromagnetics Research Letters*, Vol. 90, 113–119, 2020.
12. Holma, H. and A. Toskala, *LTE for UMTS: OFDMA and SC-FDMA Based Radio Access*, 267, John Wiley & Sons Ltd., United Kingdon, 2009.
13. Goud, J. R., N. V. Koteswara Rao, and A. M. Prasad, "Design of triple band U-slot MIMO antenna for simultaneous uplink and downlink communications," *Progress In Electromagnetics Research C*, Vol. 106, 271–283, 2020.
14. Park, J., M. Rahman, and H. N. Chen, "Isolation enhancement of wide-band MIMO array antennas utilizing resistive loading," *IEEE Access*, Vol. 7, 81020–81026, 2019, doi: 10.1109/ACCESS.2019.2923330.
15. Iqbal, A., O. A. Saraereh, A. W. Ahmad, and S. Bashir, "Mutual coupling reduction using F-shaped stubs in UWB-MIMO antenna," *IEEE Access*, Vol. 6, 2755–2759, 2018, doi: 10.1109/ACCESS.2017.2785232.

16. Naderi, M., F. B. Zarrabi, F. S. Jafari, and S. Ebrahimi, "Fractal EBG structure for shielding and reducing the mutual coupling in microstrip patch antenna array," *AEU-International Journal of Electronics and Communications*, Vol. 93, 261–267, 2018, doi.org/10.1016/j.aeue.2018.06.028.
17. Babashah, H., H. R. Hassani, and S. Mohammad-Ali-Nezhad, "A compact UWB printed monopole MIMO antenna with mutual coupling reduction," *Progress In Electromagnetics Research C*, Vol. 91, 55–67, 2019.
18. Veeramani, A., A. S. Arezomand, J. Vijayakrishnan, and F. B. Zarrabi, "Compact S-shaped EBG structures for reduction of mutual coupling," *2015 Fifth International Conference on Advanced Computing & Communication Technologies*, 21–25, 2015, doi: 10.1109/ACCT.2015.112.
19. El Ouahabi, M., A. Zakriti, M. Essaaidi, A. Dkiouak, and H. Elftouh, "A miniaturized dual-band MIMO antenna with low mutual coupling for wireless applications," *Progress In Electromagnetics Research C*, Vol. 93, 93–101, 2019.
20. Mishra, A. R., *Fundamentals of Cellular Network Planning and Optimisation 2G/2.5G/3G .....Evolution to 4G*, John Wiley & Sons Ltd, 2004.
21. Blanch, S., J. Romeu, and I. Corbella, "Exact representation of antenna system diversity performance from input parameter description," *Electron. Lett.*, Vol. 39, No. 9, 705–707, 2003, doi: 10.1049/el:20030495.
22. Zhai, H., L. Xi, Y. Zang, and L. Li, "A low-profile dual-polarized high-isolation MIMO antenna arrays for wideband base-station applications," *IEEE Transactions on Antennas and Propagation*, Vol. 66, No. 1, 191–202, Jan. 2018, doi: 10.1109/TAP.2017.2776346.